2005-01-1248

Friction Stir Spot Welding of Advanced High-Strength Steels – A Feasibility Study

Z. Feng, M. L. Santella, and S. A. David
Metals and Ceramic Division, Oak Ridge National Laboratory

R.J. Steel and S. M. Packer
MegaStir Technologies

T Pan
Ford Research and Advanced Engineering, Ford Motor Company

M. Kuo and R. S. Bhatnagar
Ispat Inland Inc

ABSTRACT

An exploratory study was conducted to investigate the feasibility of friction stir spot welding advanced high-strength steel sheet metals. The fixed pin approach was used to weld 600MPa dual phase steel and 1310MPa martensitic steel. A single tool, made of polycrystalline cubic boron nitride, survived over one hundred welding trials without noticeable degradation and wear. Solid-state metallurgical bonding was produced with welding time in the range of 2 to 3 seconds, although the bonding ligament width was relatively small. The microstructures and hardness variations in the weld regions are discussed. The results from tensile-shear and cross-tensile tests are also presented.

INTRODUCTION

Friction stir spot welding (FSSW) is a new process that recently has received considerable attention from the automotive and other industries [1]. A novel variant of the “linear” friction stir welding (FSW) process, FSSW creates a spot, lap-weld without bulk melting. The appearance of the resulting weld resembles that of a resistance spot weld commonly used for auto-body assembly. The solid-state bonding and other features of the process makes it inherently attractive for body assembly and other similar applications. Today’s primary welding process for auto body structure assembly – the electric resistance spot welding (RSW) process – can be problematic for many new high-performance light weight structural materials such as Al alloys and advanced high-strength steels (AHSS) [2,3].

So far, the majority of the research and development efforts on FSSW have been on aluminum alloys. Because Al alloys are easy to deform at relatively low temperatures (below about 550°C) they are relatively easy to friction stir weld. Indeed, the development of FSSW for Al alloys has been quite successful. Mazda reported the first application of FSSW on its 2003 RX-8, a mass production car. The entire Al rear door was friction stir spot welded [4]. Other auto companies also announced introduction of FSSW to weld Al body parts.

Two distinctive variants of the FSSW process have been reported in the open literature [5-8]. The first approach, used by Mazda, employs a fixed pin tool geometry [5,7]. The protruded pin leaves a characteristic exit hole in the middle of the joint. The second approach [8] utilizes delicate relative motions of the pin and the shoulder to refill the pin hole. Based on the information available, the second approach would require relatively long processing time to accommodate the complex motions of the tool to fill the hole. In comparison, the fixed pin approach is very fast. For Al alloys, a weld can be made in less than one second [7]. Also, the welding machine and control system for the fixed pin approach is simple and easy to integrate on a high-volume mass production assembly line. Mazda reported over 90 percent operation energy savings and over 40 percent capital investment reductions when compared to the conventional resistance spot welding of Al alloys.

Today, steel is still the primary material for body structures of high-volume mass-produced cars by all major car makers. The great emphasis on safety and vehicle weight reduction to improve fuel efficiency has been driving the increased use of AHSS in automobile body construction. However, welding AHSS presents some unique technical challenges to both the steel suppliers and the auto end-users. Data available so far have indicated that resistance spot welding of AHSS with the welding practices developed for conventional mild steels may not be the preferred approach to achieve the full benefits of AHSS. The biggest technology barrier inhibiting the use of RSW for AHSS is the profound weld property degradation [2, 9-11]. Due to the extremely high cooling rate in RSW, the weld nugget region of AHSS would develop highly brittle microstructures and is prone to solidification related weld cracks/defects. Such problems tend to be more prominent in higher grade AHSS with relatively high carbon and alloying element contents such as DP1000, Martensitic, and TRIP steels. The shortened electrode life is another major issue for RSW of AHSS because of the chemical reaction between the Zn coating and the copper electrode and high welding force. Alternative welding processes that minimize the weld property degradation without adversely affecting the productivity of body assembling would be extremely important to fully realize the advantages of AHSS in structure safety and fuel efficiency.

The success of FSSW in Al alloy body structures has led to tremendous interests in applying the technology to weld advanced high strength steels. However, past research and development on linear friction stir welding have shown that steels are much more difficult to friction stir weld than Al alloys [12]. The technical difficulties stem from the very fundamental aspect of the FSW process – compared to aluminum alloys, FSW of AHSS must operate at much higher temperatures and it requires much higher mechanical loading for plunging and stirring. These technical difficulties are also expected for FSSW. The high-volume, high-speed, and cost-conscious requirements of auto-body assembly lines make the development of FSSW even more challenging.

This paper presents the results of a feasibility study on FSSW of AHSS. While other forms of FSSW are being evaluated for welding steels and other high melting temperature materials [13], this study was based on the fixed pin approach, mainly because of its simplicity and relatively short welding time. The study was to explore the following: (1) the feasibility of producing FSSW in AHSS in a relatively short period of time acceptable to the industry, (2) the possibility of using existing tool materials for FSSW of AHSS, and (3) the microstructural responses of AHSS to the FSSW process.

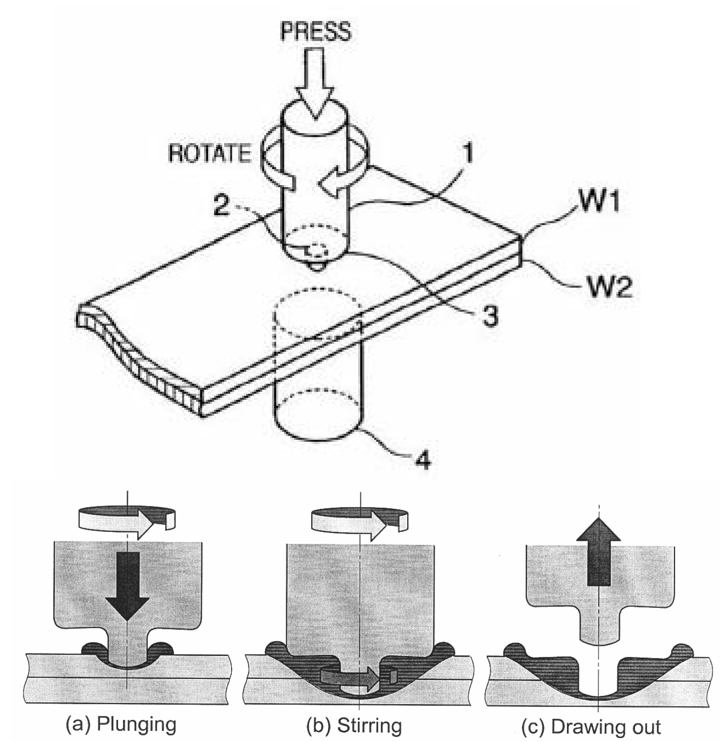

Figure 1 Principles of FSSW with fixed pin.

EXPERIMENTAL

Two types of uncoated AHSS steels were selected for this feasibility study. The first one (DP600) was a dual-phase steel with nominal strength of 600MPa, and the second one (M190) was a martensitic steel with nominal strength of 1310MPa. The thickness of the material was 1.6mm. Table 1 provides the chemical composition of the steels.

Welding trials were performed on a laboratory friction stir welding research and development system. Figure 1 illustrates the basic process of the fixed pin approach used in this study. The welding cycle begins with a rotating tool with a protruded pin plunging into the upper sheet of the lap joint. The plunge load is supported from the bottom side with a backing plate or anvil to sustain the plunging load. The heat generated by the rotating pin softens the material and facilitates the penetration of the pin. Much more heat is generated to further soften a large region of the material underneath the tool shoulder after the tool shoulder contacts the top surface of the upper sheet. The softened material is pushed and stirred to form the metallurgical bond around the rotating pin. The forge pressure from the tool shoulder also keeps the interface between the two workpieces in intimate contact to facilitate the bonding. The tool is retracted at the end, leaving the characteristic hole in the middle of the weld.

Table 1 Steel Chemistry in Wt percent

	C	Mn	P	S	Si	Cu	Ni	Mo	Cr	Cb	V	Ti
DP600	0.084	0.94	0.011	0.006	0.313	0.02	<0.01	<0.01	0.02	<0.003	0.004	0.004
M-190	0.168	0.4	0.009	0.005	0.169	0.036	0.013	0.003	0.023	<0.003	<0.003	0.034

All welds were made under displacement control mode – the tool was plunged into the material to a pre-determined depth. For all the tests conducted in this feasibility study, the tool rotation speed was fixed at 1500 rpm. The total welding time varied from 1.6 sec to 3.2 sec through changes in the plunge rate.

The tool had a tapered pin. It was 2.0-mm long. The shoulder of the tool was 10 mm in diameter.

As in the case of the linear friction stir welding, tool material is expected to be a critical technical issue for FSSW. In this work, the tool was made of polycrystalline cubic boron nitride (PCBN), a material that has been successfully used for linear friction stir welding of steel and other high melting temperature materials [14]. A single tool was used in this study. This single tool made over one hundred welds without any noticeable degradation or wear.

Tensile-shear and cross-tension mechanical testing were performed for selected welding conditions to evaluate the mechanical strength of the joints produced in this work. The tensile shear specimen was 38.1-mm wide and 127-mm long. The cross-tension specimen was 50.8-mm wide and 152.4-mm long, with the distance between the loading holes at 101.6 mm. The weld was made at the center of the overlapping (38 mm) region, as shown in Figure 2.

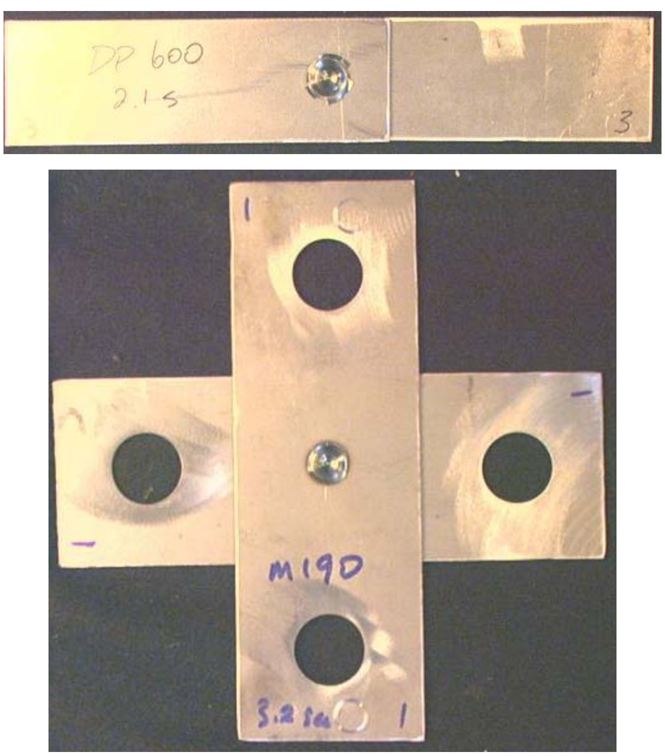

Figure 2 Appearances of the tensile shear and the cross-tension welded coupons. The welds were at the center of the overlapping region.

RESULTS AND DISCUSSIONS

Figure 3 shows the overall cross-sectional views of both the M190 weld and DP600 weld made with 2.1 sec welding time. A close-up view in the bonding interface region of the M190 weld is given in Figure 4. Clearly, metallurgical bonding was formed between the top and bottom workpieces around the penetrating pin. As in the case of Al alloy welds, the material from the bottom piece was pushed up by the plunging action of the rotating pin, causing the workpiece interface to bend upward and form a “hook”. The solid-state phase transformations that occur in carbon steels during cooling make it difficult to directly observe details of the stirring/mixing of the material between the two sheets. The width of the bonding ligament, a critical factor determining the strength of the weld, was relatively small in this study. Additional efforts would be needed to further improve the size of bond ligament.

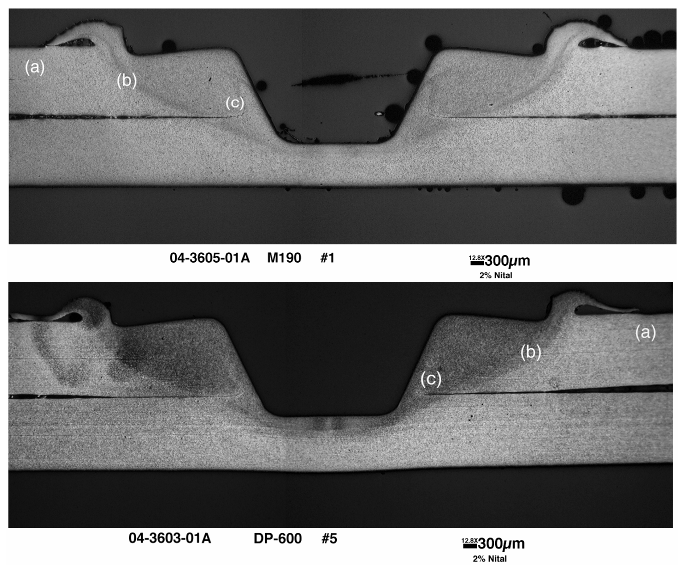

Figure 3 Cross-section of FSSW. Top: M-19; bottom: DP600. Welding time: 2.1 sec.

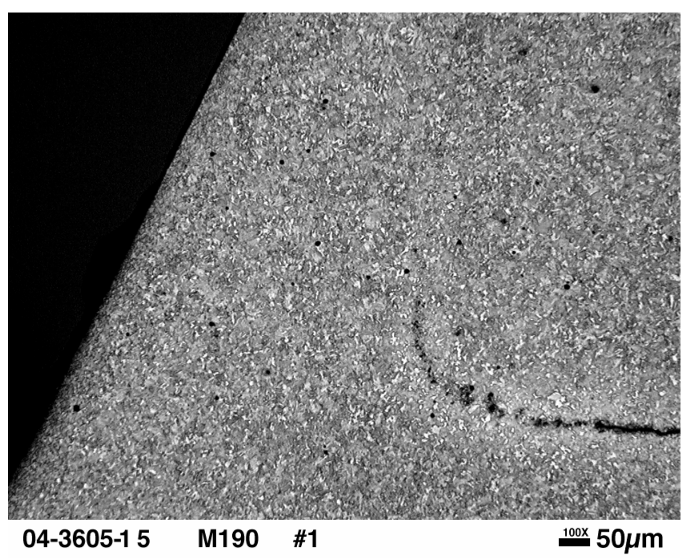

Figure 4 Close section view of the bonding interface region. M190 Steel, welding time: 2.1 sec

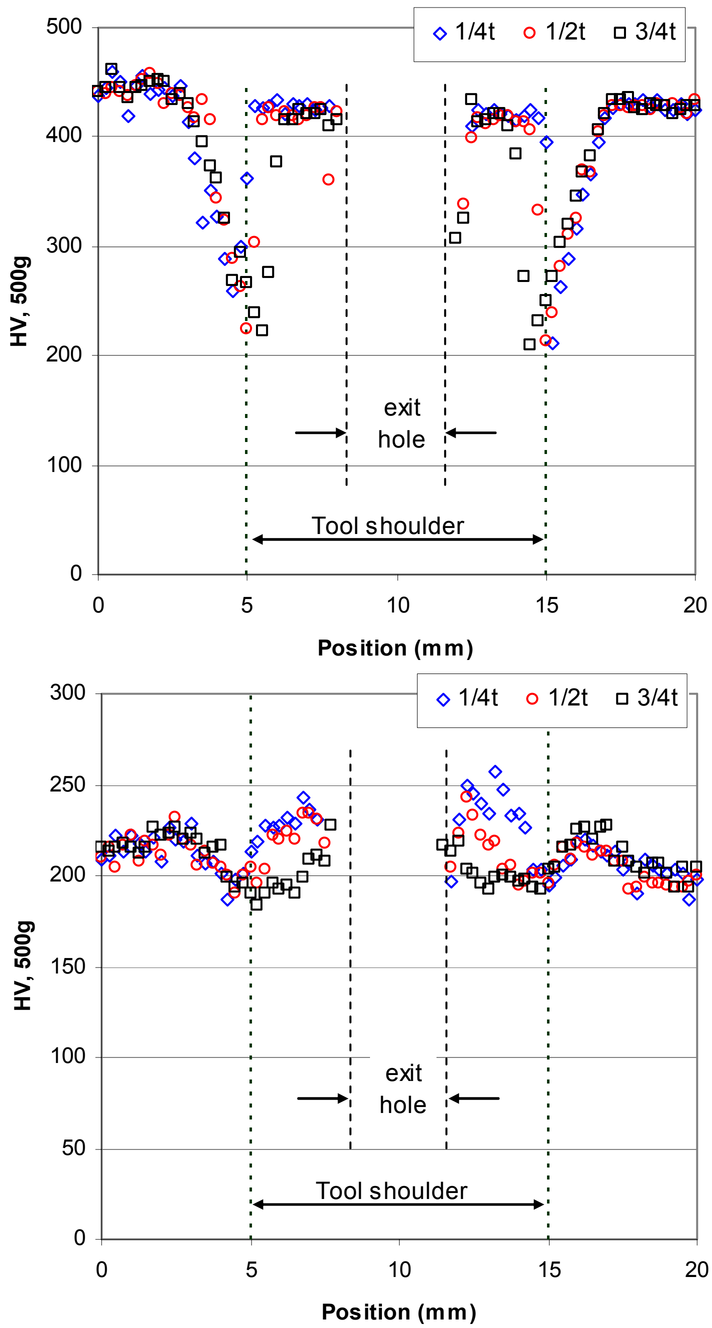

Figure 5 Micro-hardness distribution across the weld in top sheet. Top: M190; bottom: DP600. Welding time: 2.1 sec.

To evaluate the effects of welding thermal cycle on the properties of the welds, variations in the microhardness were measured across them. Figure 5 shows the microhardness distributions in the top workpiece at three different depths, approximately ¼ (0.4mm), ½ (0.8mm), and ¾ (1.2 mm) of the plate thickness, as measured from the top surface. They are labeled as ¼t, ½t, and ¾t in the figure. The location of the exit hole and the periphery of the tool shoulder are also illustrated in the figure to provide the spatial reference for the discussion of the hardness variations.

The martensitic M190 weld shows considerable softening outside the stir zone. The minimum hardness, about 200 Hv, was located about 5-mm away from the weld center, corresponding to the shoulder radius of the tool. However, the hardness in the stir zone was fully recovered back to the 430 Hv base metal level. It is important to point out that the minimum hardness location is quite far away from the bonding region at the interface. The softened region was outside the thermomechanically affected zone (TMAZ) where substantial plastic deformation and material flow occur during the welding process.

Due to the differences in chemistry, DP600 steel showed very different microhardness profiles under the same welding condition. The softening, while still measurable, was relatively insignificant compared to the base metal microhardness level. The softening was mostly outside the shoulder diameter, particularly for the ¼ t and ½ t depth. On the other hand, the stir zone appeared to be hardened. The maximum hardness was about 250Hv, compared to the base metal average of 210 Hv.

The above variations of the microhardness can be related to the microstructural changes in the different regions of the weld. While more detailed microstructural analyses are still on-going, the results obtained so far from the optical microstructure evaluation are presented below to help understand the hardness changes in the AHSS welds produced by FSSW.

Figure 6 and Figure 7 show, respectively, the microstructures at three selected representative locations in the M190 and DP600 welds. The locations of these metallographic photos are schematically illustrated in Figure 3 by the corresponding labels. Label (a) indicates the base metal region, (b) the transition region exhibiting the reduction of hardness, and (c) the region near the bonding interface which is inside the TMAZ.

The base metal of the martensitic M190 steel has a martensitic microstructure (Figure 6(a)). In the transition region located near the periphery of the tool shoulder, the material appeared to be heated to a peak temperature between the A1 and A3 temperature – the so-called intercritical region where the ferrite and austenite co-exist at the peak temperature. While the austenite will transform back to martensite on cooling, the ferrite remains. This results in a dual-phase (ferrite + martensite) microstructure in the intercritical region of the weld (Figure 6(b)). The formation of the ferrite phase hence reduces the hardness from that of the complete martensite microstructure of the base metal. Outside this intercritical region, the material would experience a peak temperature below the A1 temperature. There the metastable martensite microstructure would decompose to a more stable ferrite+Fe_3C microstructure, which also would reduce the hardness. In the TMAZ (labeled as (c) in Figure 3), the material would be heated to above the A3 temperature. The material in the TMAZ would therefore be fully austenitized on heating and transformed back to martensite due to the high hardenability of the martensitic steel. Consequently, the hardness of the

TMAZ is expected to reach that of the base metal. Because the bonding region is located in the TMAZ, it would exhibit the similar microstructure and hardness of the base metal.

As shown in Figure 7(a), the base metal of the DP600 steel has a dual-phase microstructure consisting of a ferritic grain matrix and considerable amounts of the hard phase (bainite and/or martensite) islands mostly decorating the boundaries of the ferrite grains. In the transition region (Figure 7(b)), the hardened phase region undergoes phase transformation to form fine grained structures. The resultant microstructure in this region is a network of fine grained microstructure surrounding the large ferritic grains. As in the case of M190 weld, it is expected that the peak temperature in this region falls within the intercritical temperature range to form a mixture of austenite and ferrite on heating. The austenite then transforms back to hard phases on cooling. The details of these fine grained structures would not be resolved under the optical microscope. In the TMAZ, the material is expected to be fully austenitized on heating. Due to the relatively high hardenability of DP600 steel, an increased amount of bainite/acicular ferrite was formed on cooling, resulting in the increase in the hardness in TMAZ.

The above results suggest that, for the two advanced high-strength steels studied, the FSSW process was able to maintain, to a great extent, the hardness and the microstructure of the base metal *in the bonding interface region*. This could be attributed to the combination of moderate cooling rate [13] associated with the FSSW process (compared to RSW) and the relatively high hardendability of AHSS. This provides the technical basis for further refinement and optimization of the FSSW process to control or maintain the microstructure and properties in the bonding region of the AHSS weld.

The resulting microstructure in the bonded region also suggests the material flow and bonding takes place when the material is fully austenitized. Such information would be important for the future process and tool material development for FSSW of AHSS.

Figure 8 shows the peak loads measured by the tensile shear test. Each data point represents the average of three samples made under the same welding and material conditions. For both DP600 and M190 steel, an increase in welding time from 2.1 to 3.2 seconds resulted in increases in the peak load strength. This correlated well with the increased bonding ligament width developed in the longer welding time conditions. The cross-tension testing results are presented in Figure 9, for the 3.2 welding time condition.

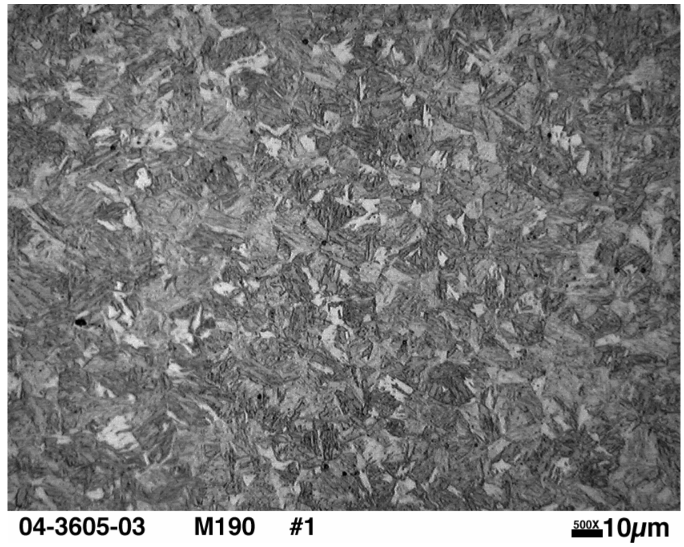

(a)

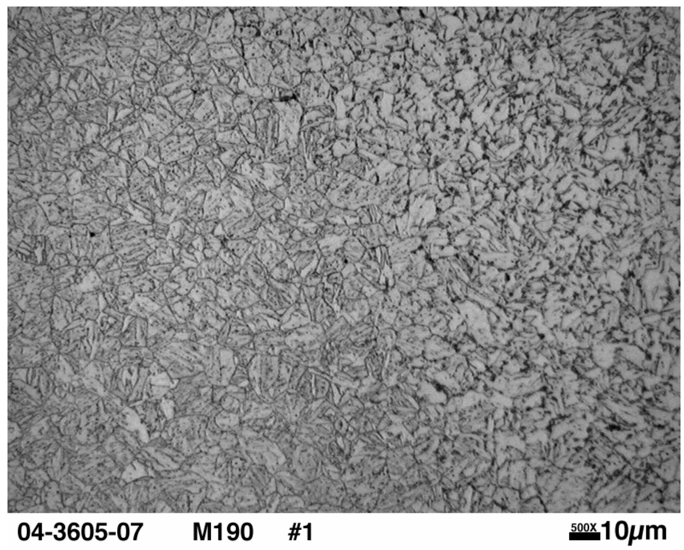

(b)

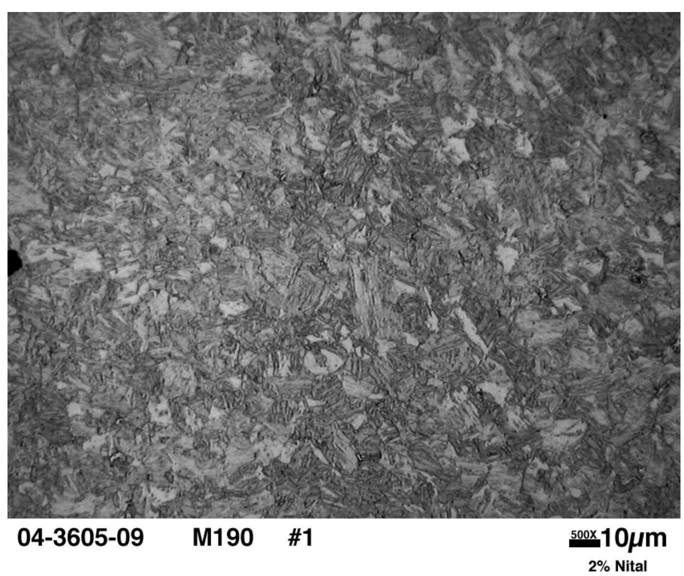

(c)

Figure 6 M190, 2.1 sec (a) Base metal, (b) transition BM to intercritical region (on the right side of the photo), (3) TMAZ. The locations are given in Figure 3.

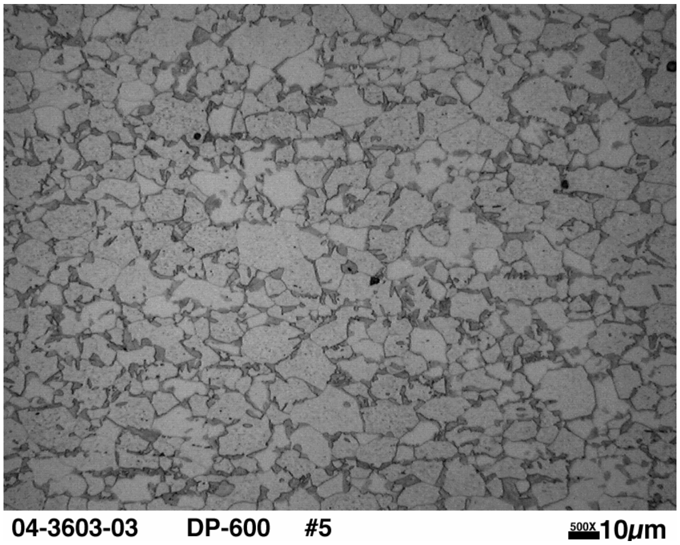

(a)

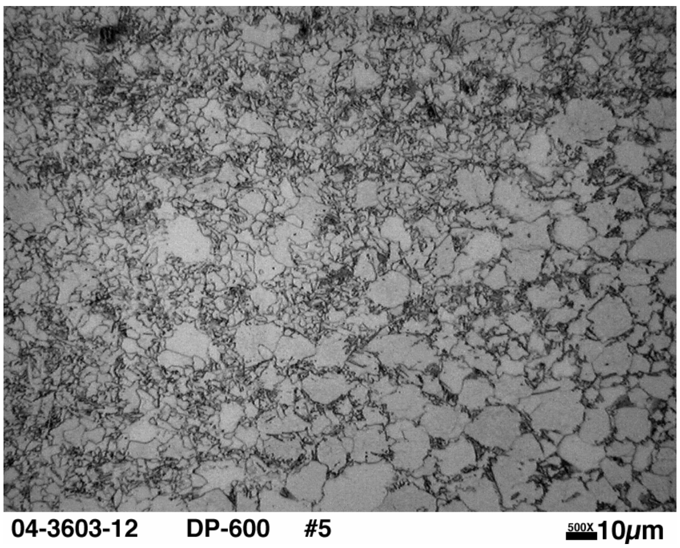

(b)

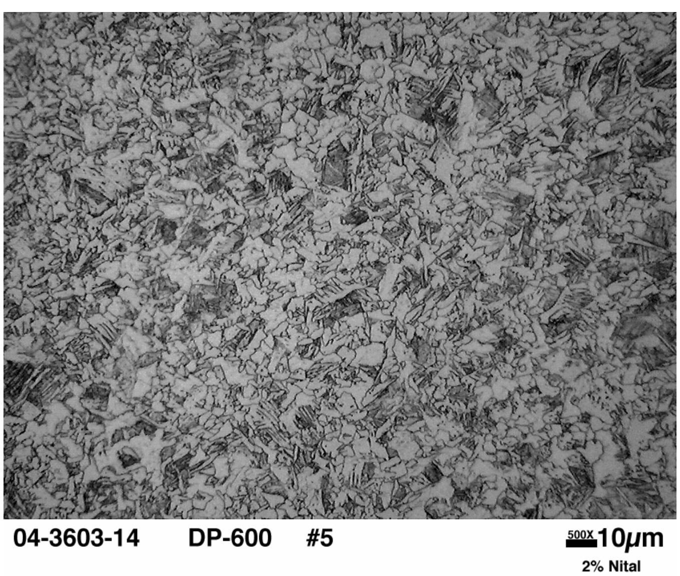

(c)

Figure 7 DP600. (a) base metal, (b) Transition from BM to the inter-critical region (on the left side of the photo), (3) TMAZ. The locations are given in Figure 3.

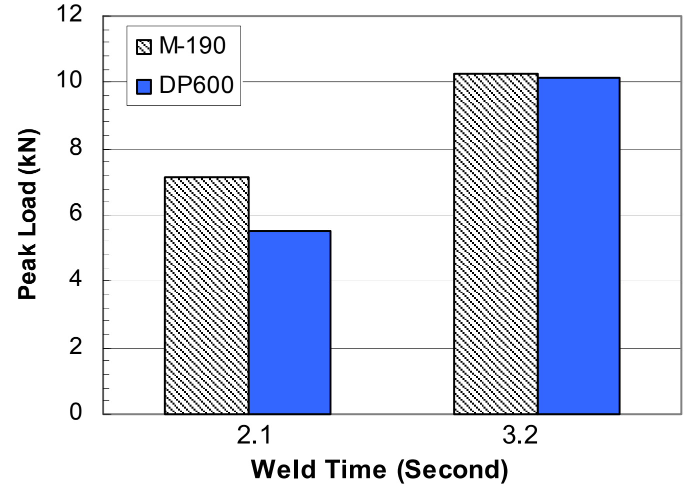

Figure 8 Peak loads from tensile shear test.

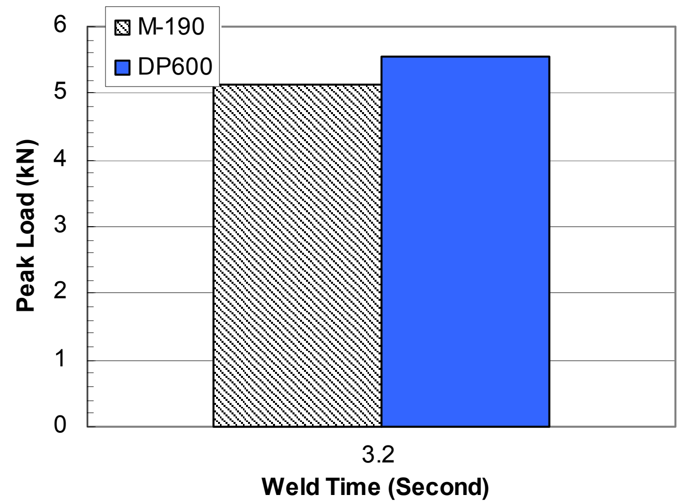

Figure 9 Peak loads from cross-tension test

It should be pointed out that only small bonding ligament widths were obtained in this feasibility study. As the bonding ligament width is a controlling factor for the strength of the joint, it is expected that substantial improvement in joint strength can be achieved if the bonding ligament width can be increased through further process development and modifications to the tool geometry.

CONCLUSION

This study investigated the feasibility of friction stir spot welding advanced high-strength steel sheet metal for automotive applications. It was found that:

1. It is possible to use the fixed pin approach to produce metallurgical bonding for both DP600 dual phase steel and M190 martensitic steel under 3 seconds of welding time.
2. The PCBN tool material was capable of producing over a hundred welds without noticeable wear and degradation.
3. The bonding region, located in the TMAZ, exhibited similar microstructure and hardness as in the base metal for both steels studied.

4. The M190 steel showed considerable softening. However, this softened region is far away from the bonding region where the failure occurred during the mechanical testing.
5. The welding process conditions used in this study produced relatively small bonding ligament widths, thereby limiting the tensile strength levels of the joint. It is expected that substantial improvement in joint strength can be achieved if the bonding ligament width can be increased through further process development and modifications to the tool geometry.

ACKNOWLEDGMENTS

This research was sponsored in part by the U.S. Department of Energy, Assistant Secretary for Energy Efficiency and Renewable Energy, Office of FreedomCAR and Vehicle Technologies, as part of High Strength Weight Reduction Materials Program under Contract DE-AC05-00OR22725 with UT-Battelle, LLC. The authors also acknowledge the supports from MegaStir Technologies, Ispat Inland Inc, and Ford Motor Company, and are grateful to A. Joaquin of Ford Motor Company for assistance with mechanical testing.

REFERENCES

1 Hancock, R., 2004, "Friction welding of Aluminum Cuts Energy Cost by 99%," *Welding Journal*, vol. 83, pp. 40.

2 Shi, S.G. and Westgate, S.A., 2003, “Resistance spot welding of high-strength steel sheet,” Corporate Research Program Report No 767/2003, The Welding Institute, Cambridge, UK.

3 Spinella, D. J., Brockenbrough, J. R., and Fridy, J. M., 2005, "Trends in Aluminum Resistance Spot Welding for the Automotive Industry," *Welding Journal*, 84(1), 34-40.

4 "*Mazda Develops World's First Aluminum Joining Technology Using Friction Heat*", Mazda News Release, February 27, 2003, http://www.mazda.com/publicity/release/200302/0227e.html.

5 Iwashita, T. "Method and Apparatus for Joining." US Patent 6601751 B2, Aug. 5, 2003.

6 Sakano, R., Murakami, K., Yamashita, K., Hyoe, T., Fujimoto, M., Inuzuka, M., Nagao, Y. and Kashiki, H., 2001, "Development of Spot FSW Robot System for Automobile Body Members," Proc. 3rd International Symposium of Friction Stir Welding, Kobe, Japan.

7 Pan, T., Joaquin, A., Wilkosz, D. E., Reatherford, L., Nicholson, J. M., Feng, Z., and Santella, M. L., 2004, "Spot Friction Welding for Sheet Aluminum Joining," Proc. 5th International Symposium on Friction Stir Welding, Metz, France.

8 Allen, C. D., and Arbegast, W. J., 2005, "Evaluation of Friction Stir Spot Welds in 2024 Aluminum," SAE Technical Paper No 2005-01-1252, Society of Automotive Engineers.

9 Ferrasse, S. Verrier, P and Meesemeacker, F, 1998, “Resistance spot weldability of high-strength steels for use in car industry,” Welding in the World, 41(2), p177-195.

10 Yamazki, K, Sato, K, and Tukunaga, 2000, “Static and fatigue strength of spot welded joint in ultra-high-strength, cold-rolled steel sheets,” Welding International, 14(7), p533-541.

11 Peterson, W, 1997, “Dilution of weld metal to eliminate interfacial fractures of spot welds in high and ultra-high strength steels,” Proc. Int. Conf Advances in Welding Technology, Columbus, 17-19, Sept, 1997, p331-346.

12 Gould, J.E., Lienert, T.J. and Feng, Z., 1998, “Recent developments in friction stir welding,” SAE Technical Paper Series 981875

13 “Development of Friction Stir Spot Welding Process,” ORNL Internal Research, 2004.

14 Packer, S. M., Nelson, T. W., Sorensen, C. D., Steel, R., and Matsunaga, M., 2003, "Tool and Equipment Requirements for Friction Stir Welding Ferrous and Other High Melting Temperature Alloys." *4th International Symposium on Friction Stir Welding*, Park City, Utah.

CONTACT

Dr. Zhili Feng, Oak Ridge National Laboratory, Metals and Ceramics Division, PO Box 2008, MS6095, Oak Ridge, TN, 37831-6095. fengz@ornl.gov